

## Article

# The Role of Chemical Activation in Strengthening Iron Ore Tailings Supplementary Cementitious Materials

Zhihang Hu <sup>1,2,3</sup>, Xiaowei Gu <sup>1,2,3,\*</sup>, Baojun Cheng <sup>1,4</sup>, Qing Wang <sup>1,2,3</sup>, Jianping Liu <sup>5,\*</sup>, Xiaowei Ge <sup>1,2,3</sup>   
and Shiqi Yin <sup>1,2,3</sup>

<sup>1</sup> School of Resources and Civil Engineering, Northeastern University, Shenyang 110819, China

<sup>2</sup> Science and Technology Innovation Center of Smart Water and Resource Environment, Northeastern University, Shenyang 110819, China

<sup>3</sup> Liaoning Institute of Technological Innovation in Solid Waste Utilization, Shenyang 110819, China

<sup>4</sup> China West Construction Building Materials Science Research Institute, Chengdu 610221, China

<sup>5</sup> School of Architecture and Civil Engineering, Shenyang University of Technology, Shenyang 110870, China

\* Correspondence: guxiaowei@mail.neu.edu.cn (X.G.); liujianping024@163.com (J.L.)

**Abstract:** The preparation of iron ore tailings (IOTs) into supplementary cementitious materials (SCMs) is an effective approach to achieve value-added utilization of industrial solid waste. This study systematically investigates the hydration pattern and strength development of Portland cement systems with the incorporation of IOTs, steel slag (SS), granulated blast-furnace slag (GBFS), and fly ash (FA) under the action of different chemical additives. The hydration products, and microstructure and pore structure of the SCMs are analyzed using X-ray diffraction, Fourier transform infrared spectroscopy, scanning electron microscopy, and mercury intrusion porosimetry. The findings of this study demonstrate that chemical activation plays a significant role in the strength development of SCMs. Among the five chemical activators tested, Triethanolamine (TEA) had the greatest influence on mechanical properties. The maximum compressive strength of the SCMs at 28 days was 42.9 MPa at a dosage of 1%. Specifically, the addition of TEA promotes volcanic ash reactions, and the high fineness of SCM provides nucleation sites for hydration products. Interactions between the volcanic ash reaction and the complexation reaction of TEA have a positive effect on compressive strength development. This research expands the potential for IOTs SCMs through chemical activation methods for value-added applications.

**Keywords:** iron ore tailing; supplementary cementitious materials; chemical activation; triethanolamine; strength development



**Citation:** Hu, Z.; Gu, X.; Cheng, B.; Wang, Q.; Liu, J.; Ge, X.; Yin, S. The Role of Chemical Activation in Strengthening Iron Ore Tailings Supplementary Cementitious Materials. *Buildings* **2024**, *14*, 963. <https://doi.org/10.3390/buildings14040963>

Academic Editor: Xiaoyong Wang

Received: 26 January 2024

Revised: 7 March 2024

Accepted: 25 March 2024

Published: 1 April 2024



**Copyright:** © 2024 by the authors. Licensee MDPI, Basel, Switzerland. This article is an open access article distributed under the terms and conditions of the Creative Commons Attribution (CC BY) license (<https://creativecommons.org/licenses/by/4.0/>).

## 1. Introduction

Iron is an indispensable resource for humans, playing a crucial role in the development of industrialization through the use and innovation of iron-based materials like steel. However, this reliance on iron necessitates large-scale mining and refining, leading to numerous ecological problems [1]. Additionally, IOTs, a byproduct of mining, present significant environmental risks, including water and atmospheric contamination and metal ion leaching. Approximately 600 million tons of IOTs are estimated to be generated annually in China [2], with reports suggesting over 1.2 billion tons produced in 2020 [3]. The utilization of this solid waste is minimal, resulting in most being stored in extensive yards, evidenced by over 14,000 tailing dams in China [4].

In recent years, there has been a growing emphasis on the recycling of IOTs, with an increasing number of disposal methods being proposed. Currently, integrating IOTs into cement-based materials appears to be the most promising approach for large-scale utilization. The shortage of natural sand and the high silicon content of most IOTs have led to numerous studies focusing on the development of IOTs as aggregates. IOTs sand, possessing a fineness akin to natural sand, can be effectively recycled as a fine aggregate in

concrete [5]. Additionally, large-particle stripped iron ore waste rock shows potential as a coarse aggregate [2]. However, challenges arise with finer powdered IOTs, which are prone to creating environmental concerns, such as dust generation. These powdered materials can also be incorporated into cement, acting as supplementary cementitious materials (SCMs) [6,7]. Replacing a portion of the cement in concrete with IOTs is also feasible, reducing the need for clinker and enhancing the eco-friendliness of the materials, which leads to additional environmental benefits [8]. SCMs come in various forms, predominantly based on a  $\text{CaO-Al}_2\text{O}_3\text{-SiO}_2$  matrix [9]. Due to the synergistic effect between the materials, the replacement level of composite SCMs to cement could reach more than 30% with almost no adverse effect on the performance [10]. However, despite their inherent potential for reactivity, many SCMs, including those derived from IOTs, exhibit unexpectedly low reactivity in cementitious systems. This discrepancy presents challenges in quantifying their impact on cement hydration [11]. The incorporation of IOTs into Portland cement leads to a complex system, where the typical hydration of Portland cement is influenced by both the physical and chemical characteristics of the SCMs, which may include limited pozzolanic activity [12].

While it seems that IOTs of all particle sizes can be readily recycled into cementitious materials, the practical reuse of IOTs powder is impeded by its low reactivity within such systems. IOTs are highly crystalline, composed primarily of mineral phases like  $\alpha$ -quartz and hematite, which have been shown to be nearly inert in many studies [13]. Although mechanical activation has been reported to enhance the pozzolanic activity of IOTs, thus improving the performance of IOT-based cementitious systems [14,15], Duarte et al. [16] found that mechanically activated IOTs did not exhibit volcanic ash activity, suggesting a predominant nucleation effect. Undoubtedly, mechanical activation is an effective method to treat IOTs, but it is inconclusive whether IOTs only play a physical role as fillers, or are also involved in the pozzolanic reaction. Despite the numerous benefits of mechanical activation, the mechanical properties of cementitious materials incorporating IOTs are still unsatisfactory. In particular, the strength of binders decreases dramatically when the proportion of IOTs is large [17]. While the addition of IOTs in small quantities is feasible, it may not fulfill the original purpose of researching SCMs, which were actually developed and applied to reduce clinker usage and hence carbon emissions from cementitious materials. However, as the proportion of IOTs of approximately 10% exhibits a small impact on mechanical properties at present, the environmental benefits of doing so are negligible.

There are reports that the effect of mechanical–chemical activation of IOTs is better than that of mechanical activation [18]. Chemical activation can increase the specific surface area and disrupt the crystal structure of IOTs, stimulating the potential volcanic ash activity of IOTs to meet the requirements of volcanic ash activity [14]. Chemical activation results in the production of a greater amount of amorphous material in the IOTs compared to single wet mill activation. This leads to a more significant reduction in the surface binding energy of the chemical bonds within the IOT, which further enhances the activity of the IOTs [19]. Carvalho [20] developed a geopolymer using IOTs as a geopolymer precursor, and phosphoric acid ( $\text{H}_3\text{PO}_4$ ) as an activating agent responsible for resistance gain. Alkali activators such as hydroxides, silicates, carbonates, alkali metal oxides, and aluminum sulphate are generally effective when used alone [21]. Triethanolamine (TEA) is an important chemical admixture in cementitious materials that acts as a cement grinding aid, regulates setting time, and is a component of early strength enhancers [22]. Previous studies have revealed that TEA can accelerate the pozzolanic reaction rate of SCMs to some extent [23,24]. At a concentration of 1.0%, TEA has a significant accelerating effect on cementitious materials [25]. Furthermore, as a crucial component of the cement industry, chemical additives are frequently employed to regulate the characteristics of cement. These additives consist of diverse functional groups and chemical constituents that engage in the hydration process of cement, resulting in modifications in the binding and cement-solidifying properties of the substance [26]. The incorporation of supplementary cementitious materials (SCMs)

induces changes in certain attributes of the cement, impeding the desired impact of chemical additives in composite cements. Additionally, the efficacy of chemical additives is influenced by the type of composite cement, presenting an additional obstacle in their effective implementation [27]. The impact of various chemical activators, and their dosages, on the performance of IOTs in SCM is uncertain.

Therefore, this paper aims to explore two issues in the resource utilization of IOTs: (1) the role of chemically activated IOTs in cementitious materials; and (2) the effect of different chemical additive types and dosages on the properties of cementitious materials. First, the variation of IOTs themselves and IOTs paste with different degrees of chemical activation was investigated. Subsequently, considering the disposal of industrial solid waste, composite SCMs, composed of SS, FA, and GBFS, were proposed to improve the performance of the IOTs mortar. Finally, the effect of composite SCMs on the hydration of IOTs paste was studied in depth. This study further promotes the understanding of mechanochemical activation of IOTs and enables the recycling of multiple solid wastes through the development of composite SCMs. Enhancing the gelling activity of IOTs and increasing its dosage is crucial for expanding the consumption of IOTs in the cement and concrete sector.

## 2. Materials and Methods

### 2.1. Raw Materials

Ordinary Portland cement (OPC 42.5) was employed in this study. IOTs, SS, FA, and GBFS were used as SCMs. The chemical composition of the cementitious materials is presented in Table 1. It can be seen that the IOTs present a high  $\text{SiO}_2$  content and belong to a high-silica type of IOTs.  $\text{Na}_2\text{SiO}_3$ ,  $\text{Na}_2\text{SO}_4$ ,  $\text{NaOH}$ ,  $\text{Ca}(\text{OH})_2$ , and TEA were used as chemical activators to activate IOTs. Table 1 shows the chemical compositions of PC, IOTs, SS, FA, and GBFS. Figure 1b displays the X-ray diffraction patterns of the raw materials. The  $\text{C}_3\text{S}$  and  $\text{C}_2\text{S}$  in SS make it exhibit latent hydraulic properties [28]. Therefore, SS, FA and GBFS all have higher activity in cementitious systems, especially at the later stages of hydration. The particle size distribution of the raw materials is shown in Figure 1a. Moreover, the specific surface area of the binders is listed in Table 1.

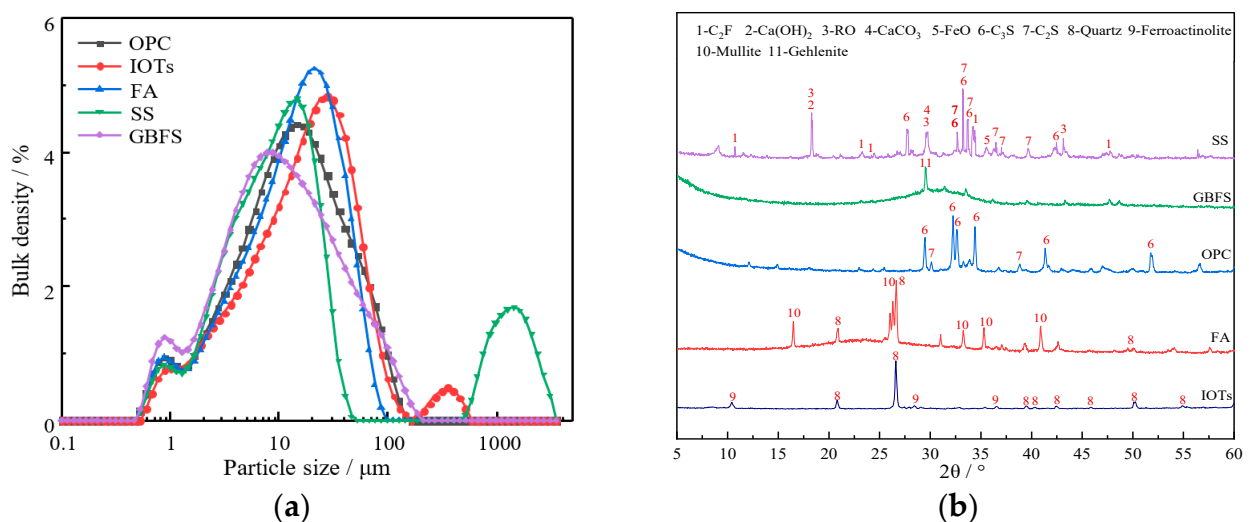


**Figure 1.** (a) Laser particle size of mineral admixture; (b) X-ray diffraction pattern of mineral admixture.

**Table 1.** Physicochemical properties of raw materials.

Chemical Composition (wt. %)	Materials				
	OPC	IOTs	SS	FA	GBFS
SiO <sub>2</sub>	28.16	70.46	15.20	60.20	34.50
Al <sub>2</sub> O <sub>3</sub>	7.44	0.91	2.53	29.39	17.70
CaO	54.86	2.68	42.65	2.49	34.00
Fe <sub>2</sub> O <sub>3</sub>	2.76	14.54	27.54	3.78	1.03
MgO	2.37	11.29	6.05	0.51	6.01
SO <sub>3</sub>	2.32	0.12	0.12	0.26	1.64
Specific surface area (m <sup>2</sup> /g)	1.01	0.83	0.97	1.02	1.23

## 2.2. Experimental Design

### 2.2.1. Mechanochemical Activation

To understand the effect of mechanochemical activation on IOTs, IOTs were milled using a ball mill, and subsequent chemical excitation with different types and dosages of chemical activators. The ball mill was operated at a frequency of 50 Hz and a power of 1.5 kW. Zirconia balls of 2–12 mm in diameter were employed as grinding media. The speed of the ball mill was maintained at 400 r/min. The ball to material ratio was fixed at 9:4. Appropriate grinding time can increase the specific surface area of IOTs. It has been shown in the literature that too long a grinding time can lead to agglomeration of the IOTs particles due to intermolecular forces, as well as wasting energy [18]. The IOTs were mechanically activated for 40 min, followed by chemical activation. Chemical activation was carried out using inorganic chemical activators, Na<sub>2</sub>SiO<sub>3</sub>, Na<sub>2</sub>SO<sub>4</sub>, NaOH, Ca(OH)<sub>2</sub>, and the organic chemical activator TEA at 0.5%, 1%, 2%, 3%, and 4% of the composite admixture, respectively. The experimental design had three samples for each different doping and chemical additive.

### 2.2.2. Sample Preparation

Prior to this study, a large number of IOTs SCMs ratio tests have been carried out. Considering the fluidity and mechanical properties of each sample, the SCMs admixture ratio was 9:6:8:4 for IOTs, SS, FA, GBFS, respectively. The mechanical properties and hydration of mortars containing 30% mechanically activated IOTs were investigated, and the mix proportion is shown in Table 2. The preparation process of the sample was as follows. The test materials were weighed according to a mix proportion of the sample. The SCMs used a water-to-cement ratio of 0.5 to produce a size of 40 mm × 40 mm × 160 mm cement mortar test blocks, at a temperature of 20 ± 1 °C, relative humidity of not less than 95% of the conditions of maintenance to 7 and 28 days. The compressive strength was determined after 7 and 28 days.

**Table 2.** The mix proportion of sample (g).

OPC	IOTs	SS	FA	GBFS	ISO Sand	Water	w/b
315	45	30	40	20	1350	225	0.5

## 2.3. Experimental Methods

Standard mortar specimens (dimensions of 40 × 40 × 160 mm) were used for the compressive strength test. Each mix sample was subjected to six compressive strength tests. X-ray diffraction (XRD) is an effective tool for identifying crystalline phases in IOTs and hydrated IOTs paste. The XRD test was carried out at a current of 40 mA, a voltage of 40 kV, and a scanning speed of 5°/min (the instrument was a Rigaku Ultima IV diffractometer from Rigaku, Japan, Cu Kα). All specimens were scanned in the range of 5° to 90°. For the hydrated samples, they were soaked in anhydrous ethanol for 7 days to stop the

hydration. They were then ground to a powder of less than 75  $\mu\text{m}$  for XRD test. The sample preparation for thermogravimetry (TG) was the same as for XRD, i.e., termination of hydration followed by grinding into powder. 30–1000  $^{\circ}\text{C}$  was selected as the test interval for TG, with a heating rate of 20  $^{\circ}\text{C}/\text{min}$ . The test was performed at a constant ambient temperature and under a nitrogen atmosphere. The structure of the hydration products was probed by Fourier transform infrared (FTIR) tests. The test range was 400–4000  $\text{cm}^{-1}$ . A Zeiss Sigma 300 scanning electron microscope (SEM), and the manufacturer is Carl Zeiss AG, Oberkochen, Germany, was employed to study the microscopic morphology of IOTs cementitious materials. Mercury intrusion porosimetry (MIP) is recognized as an effective means to examine the pore structure of cement-based materials. In this study, the microstructure of IOTs mortar was explored by mercury piezometer Microactive Autopore V 9600, and the manufacturer is Micromeritics Instruments Corporation, Norcross, GA, USA. The pressure range of MIP was 0–414 MPa.

### 3. Results

#### 3.1. Compressive Strength of IOTs

##### 3.1.1. Inorganic Chemical Activator Dosage Effect

Chemical activation agents include  $\text{Na}_2\text{SiO}_3$ ,  $\text{Na}_2\text{SO}_4$ ,  $\text{NaOH}$ ,  $\text{Ca}(\text{OH})_2$ , and TEA. Different concentrations of these agents (0.5%, 1%, 2%, 3%, 4%) were combined with IOTs and subjected to mechanical grinding for 40 min. This study investigated the effect of mechanical–chemical activation on the mechanical properties of IOTs SCMs. Figure 2 illustrates the compressive strength of samples treated with varying concentrations of chemical activators, measured after curing for 7 and 28 days. The effect of all four inorganic chemical admixtures,  $\text{Na}_2\text{SiO}_3$ ,  $\text{Na}_2\text{SO}_4$ ,  $\text{NaOH}$ , and  $\text{Ca}(\text{OH})_2$ , improved the initial strength of the samples. The optimum dosage of  $\text{Na}_2\text{SiO}_3$  and  $\text{NaOH}$  was 1%, and the compressive strength at seven days was 24.1 MPa and 26 MPa, respectively, followed by a subsequent decrease in compressive strength with the further increase in chemical activator dosage. The optimum dosage of  $\text{Na}_2\text{SO}_4$  and  $\text{Ca}(\text{OH})_2$  was 2%, and their compressive strengths were 25.1 MPa and 27.1 MPa, respectively. The compressive strength of the 1%  $\text{Na}_2\text{SiO}_3$  chemically activated samples at 7 and 28 days was the highest compared to the other samples, at 24.1 MPa and 41.2 MPa, respectively. The excitation effect of  $\text{Na}_2\text{SiO}_3$  on the samples was gradually weakened when the amount of activator doping was more than 1%, and this phenomenon might be caused by the fact that excessive  $\text{Na}_2\text{SiO}_3$  excitation of samples promotes the generation of hydration products and improves the hydration of hydration products. A composite admixture promotes the generation of hydration products, improves the density of the system around the hydration products, and ultimately leads to a decrease in strength.  $\text{NaOH}$  and  $\text{Na}_2\text{SO}_4$  provided free  $\text{Na}^+$  and  $\text{SO}_4^{2-}$  in the iron tailings-based composite admixture system, which promoted the depolymerization of  $\text{SiO}_4$  and  $\text{AlO}_4$  in the IOTs SCMs system, participated in the hydration reaction to generate a hydrated C-(A)-S-H gel, and facilitated the generation of the hydration product, calcite, which accelerated the hydration reaction. For the synergistic effect between  $\text{Ca}(\text{OH})_2$  and slag in the IOTs SCMs system to occur, mechanochemical high-energy ball milling can make the slag powder rapidly fine and significantly improve the hydration activity and strength of slag, which has a very low compressive strength by itself, and then strength is significantly increased after adding  $\text{Ca}(\text{OH})_2$  [29].

##### 3.1.2. Organic Chemical Activator Dosage Effect

Figure 2 illustrates that as TEA concentration increases, the compressive strengths of the samples at 7 and 28 days initially increase before decreasing. In comparison with the five chemical admixtures discussed in Section 3.1.1, a 1% TEA dosage notably enhances the compressive strength of the iron tailings-based composite admixture, achieving 28.6 MPa at 7 days and 42.9 MPa at 28 days. The compressive strength of the TEA-activated sample at seven days was higher by 18.6%, 13.9%, 10%, and 5.5% compared to those activated with optimal doses of  $\text{Na}_2\text{SiO}_3$ ,  $\text{Na}_2\text{SO}_4$ ,  $\text{NaOH}$ , and  $\text{Ca}(\text{OH})_2$ , respectively. At 28 days,

the strength improvements were 4.1%, 6.9%, 21.5%, and 10.8%, respectively, matching the strength of OPC. The complexation reaction of TEA interacting with the pozzolanic reaction positively contributes to the development of cement strength [30]. Research indicates that the effectiveness of TEA in cement systems varies according to its concentration, serving as an accelerator at concentrations between 0.02–0.05%, and showing reduced efficacy when the concentration exceeds 0.1%. At a 1.0% concentration, TEA significantly accelerates the setting process of the cementitious material [25].

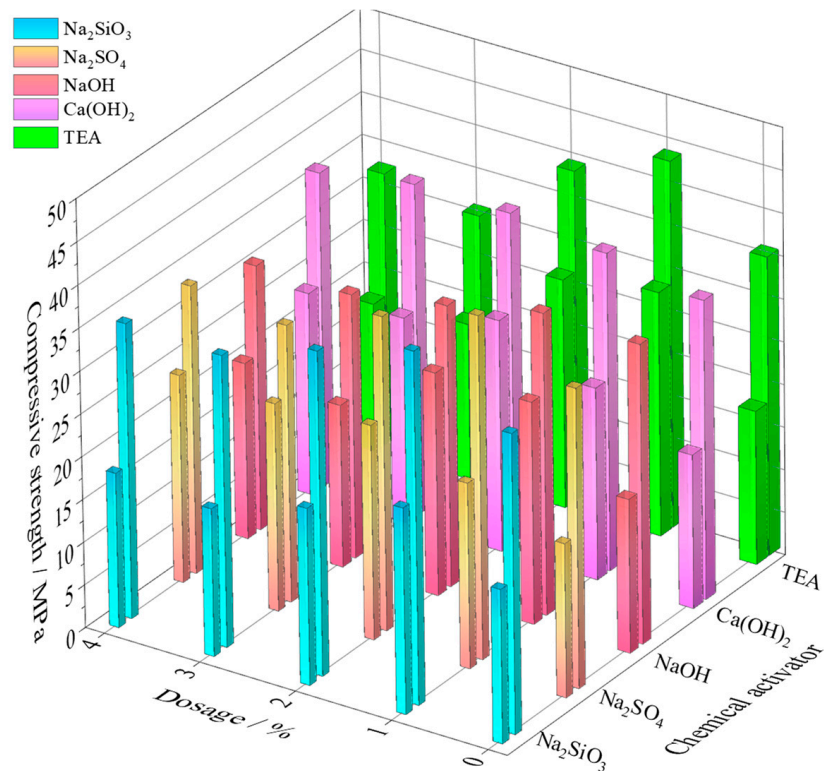


**Figure 2.** Compressive strength of samples activated by different chemical activators.

### 3.2. XRD Characterization

Figure 3 depicts the XRD data of samples after chemical activation. After seven days of chemical modification with five additives, the types of hydration products in samples remained largely unchanged. The identified hydration products included calcium hydroxide, C-S-H gel, and Hydrotalcite (Ht). After seven days, the X-ray diffraction patterns showed a significant difference in the intensity of calcium hydroxide peaks when comparing the admixture containing TEA to the other four admixtures. The calcium hydroxide peaks in the TEA-containing mixture were significantly weaker than those in the mixtures with Na<sub>2</sub>SiO<sub>3</sub>, Na<sub>2</sub>SO<sub>4</sub>, and NaOH. This suggests that when calcium hydroxide and TEA are used as chemical activators, the calcium hydroxide produced during cement hydration is significantly consumed by the active components in the admixture, resulting in a higher compressive strength when TEA is used. For the specimens at 28 days, as shown in Figure 3b, the calcium hydroxide diffraction peaks for each admixture group were significantly lower than at 7 days. This indicates a higher consumption of calcium hydroxide, more hydration products, and an increase in overall compressive strength. Additionally, the quartz content in the admixtures containing Na<sub>2</sub>SiO<sub>3</sub> and Na<sub>2</sub>SO<sub>4</sub> increased significantly.

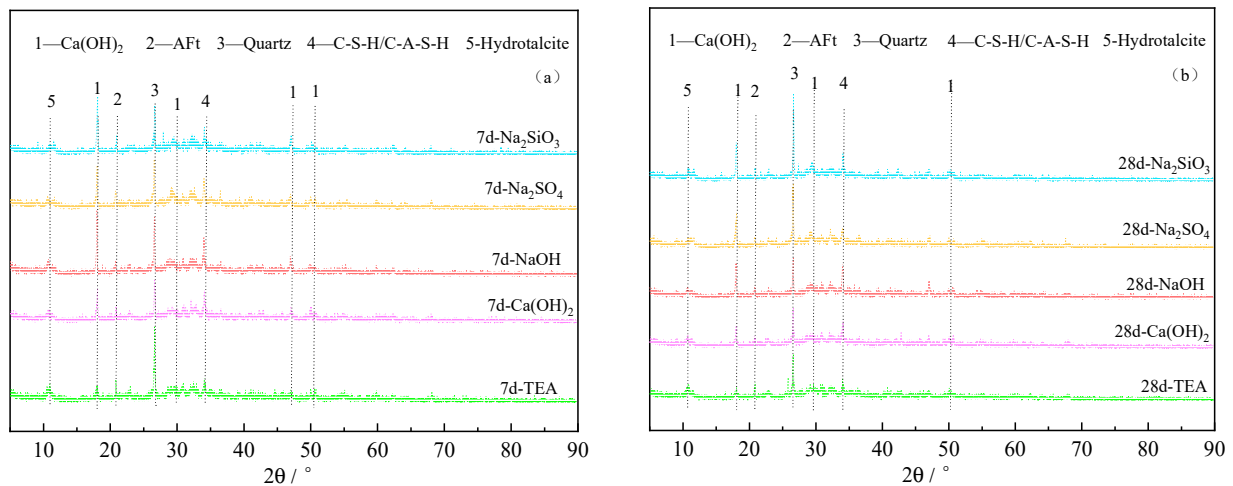


**Figure 3.** XRD pattern: (a) 7 days' XRD pattern of samples; (b) 28 days' XRD pattern of samples.

### 3.3. FTIR Analyses

The FTIR spectrums obtained for chemically modified samples for 7 and 28 days are shown in Figure 4. The vibration at  $3640\text{ cm}^{-1}$  is caused by the stretching vibration of the O-H group, indicative of the Ca(OH)<sub>2</sub> present in the material. The absorption peak at  $3460\text{ cm}^{-1}$  corresponds to the characteristic absorption of hydroxyl groups, resulting from the stretching vibration of the O-H group. O-H groups are from AFt and C-(A)-S-H gels in the sample. The figure reveals that the peaks for each admixture-modified, iron tailings-based composite are distinctly sharp, suggesting the formation of a greater quantity of amorphous gels. The peaks at  $1650\text{ cm}^{-1}$ , resulting from the bending vibration of chemically bonded water in AFt and C-(A)-S-H gels, were not prominent at 7 days but became more pronounced at 28 days. Additionally, the bending vibration at  $1650\text{ cm}^{-1}$  is attributed to the C-O bending vibration, arising from the carbonation reaction between calcium carbonate in the raw materials, the alkaline materials in the composite dopants, and the atmospheric CO<sub>2</sub>. This vibration intensity increases over time, indicating a growing presence of carbonate products in the composite admixture. The asymmetric tensile vibration at  $1000\text{ cm}^{-1}$ , identified as Si-O-T (T: Si, Al), correlates with the formation of C-(A)-S-H gel in the composite admixture. This vibration is notably stronger at 28 days compared to 7 days, suggesting an increased presence of C-(A)-S-H gel over time. The peak observed at  $450\text{ cm}^{-1}$ , which is more pronounced in the 28 days' samples, is associated with the bending vibration in the Si-O-Si network, indicative of the hydration product, C-(A)-S-H gel.

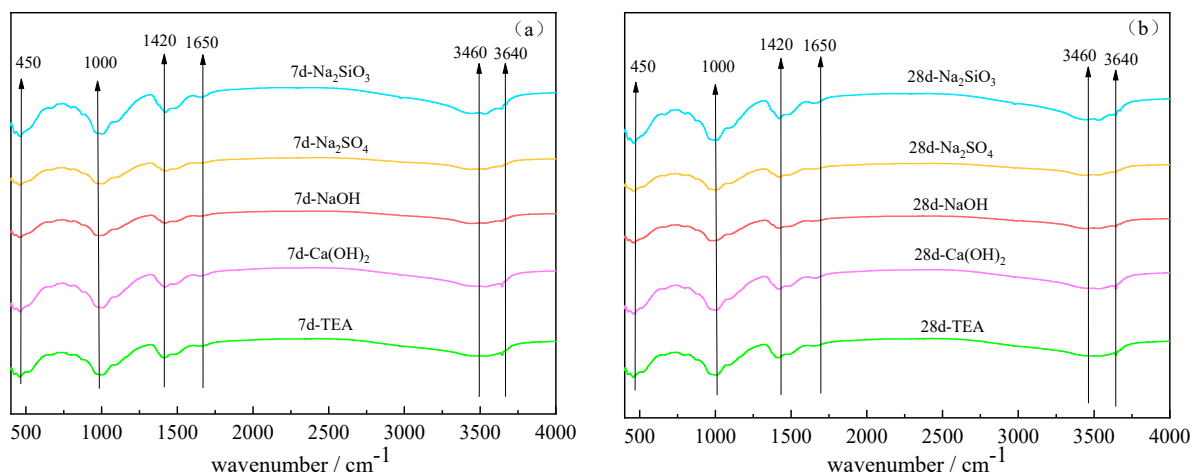


**Figure 4.** FTIR spectrum: (a) 7 days' samples; (b) 28 days' samples.

### 3.4. TG–DTG Analyses

The quantitative analysis and determination of hydration products can be achieved using the TG–DTG test, which measures their decomposition temperature. In an IOTs SCMs system, the content of calcium hydroxide (CH) decreases as a result of the secondary hydration reaction. Thus, the DTA–TG technique can be utilized to analyze the quantity of CH present in the solidified paste, thereby demonstrating the occurrence of the secondary hydration reaction. It is important to note that the rates of decomposition and dehydration of various hydrates differ at distinct temperatures [31]. The amount of this hydrate can usually be calculated by measuring the mass loss at a specific temperature. Figure 5 exhibits the thermal behavior of all specimens determined by TG–DTG. With the gradual increase in temperature, the mass loss of the iron tailings-based composite admixture simultaneously increased, and there existed four more pronounced heat absorption peaks in the DTG, mainly at 50–200 °C, 300–400 °C, 400–500 °C, and 600–800 °C, related to the dehydration of the C-(A)-S-H gel, Aft, the Ht, the calcium hydroxide, and the carbonate, respectively. In order to obtain a more comprehensive understanding of the hydration process in the composite system composed of IOTs SCMs ternary admixture system and cement, the CH content in different sample groups was determined at various stages using Equation (1) [14].

$$\text{CH} = \text{WL}_{\text{CH}} * m_{\text{CH}}/m_{\text{H}_2\text{O}} + \text{WL}_{\text{CaCO}_3} * m_{\text{CaCO}_3}/m_{\text{CO}_2} \quad (1)$$

where: CH is the relative content of calcium hydroxide in the sample; WL<sub>CH</sub> is the mass loss of calcium hydroxide; %. WL<sub>CaCO<sub>3</sub></sub> is the mass loss of calcium carbonate caused; %. m<sub>CH</sub> is the molar mass of calcium hydroxide; m<sub>H<sub>2</sub>O</sub> is the molar mass of water; m<sub>CaCO<sub>3</sub></sub> is the molar mass of calcium carbonate; m<sub>CO<sub>2</sub></sub> is the molar mass of carbon dioxide. The values of WL<sub>CH</sub> and WL<sub>CaCO<sub>3</sub></sub> can be obtained by processing the TG curve data. m<sub>CH</sub> = 74 g/mol; m<sub>H<sub>2</sub>O</sub> = 18 g/mol; calcium carbonate = 100 g/mol; m<sub>CO<sub>2</sub></sub> = 44 g/mol. The molar masses of CH, water, CaCO<sub>3</sub> and CO<sub>2</sub> can be substituted into Equation (2) [32].

$$\text{CH} = \text{WL}_{\text{CH}} * 74/18 + \text{WL}_{\text{CaCO}_3} * 100/44 \quad (2)$$

In the temperature range of 50–200 °C, the mass loss is primarily due to the dehydration of calcium aluminate crystals and C-(A)-S-H gel. Under the influence of Na<sub>2</sub>SiO<sub>3</sub>, Na<sub>2</sub>SO<sub>4</sub>, NaOH, Ca(OH)<sub>2</sub>, and triethanolamine, the mass losses are observed to be 8.92%, 8.95%, 8.92%, 9.34%, and 9.53%, respectively. Between 300–400 °C, the main mass loss occurs due to the dehydration of Ht. The mass losses associated with the dopants under the influence of Na<sub>2</sub>SiO<sub>3</sub>, Na<sub>2</sub>SO<sub>4</sub>, NaOH, Ca(OH)<sub>2</sub>, and TEA are 1.85%, 1.87%, 1.89%, 2.12%, and 2.04%, respectively. In the 400–600 °C range, the mass loss is due to the dehydration of calcium hydroxide. Under the influence of Na<sub>2</sub>SiO<sub>3</sub>, Na<sub>2</sub>SO<sub>4</sub>, NaOH, Ca(OH)<sub>2</sub>, and TEA, the mass losses in the composite admixture are 2.92%, 2.81%, 3.07%, 3.15%, and 2.66%, respectively. Between 600–800 °C, the predominant mass loss is attributed to the dehydration of carbonates. The mass losses in the composite admixture under the influence of the five different chemical activators—Na<sub>2</sub>SiO<sub>3</sub>, Na<sub>2</sub>SO<sub>4</sub>, NaOH, Ca(OH)<sub>2</sub>, and TEA—are 3.01%, 2.70%, 2.73%, 3.27%, and 2.90%, respectively.

The reactivity of calcium hydroxide with the mineral admixtures depends on the amount of calcium hydroxide and the degree of hydration of the mineral admixture. There is a positive correlation between Ca(OH)<sub>2</sub> content and the degree of hydration in cement paste, as indicated by reference [33]. Table 3 presents the content of non-evaporated water and Ca(OH)<sub>2</sub> in the hydration products under various chemical admixtures. When TEA was used to activate the IOTs SCMs system, the greatest weight loss and formation of C-(A)-S-H gels occurred at 50–200 °C. This is further demonstrated by the highest compressive strength achieved at 28 days when chemically activating the sample with TEA. Additionally, the lowest weight loss was observed at 400–500 °C, which is consistent with the 28-day XRD results. This suggests that in the presence of TEA, more Ca(OH)<sub>2</sub> was consumed in

the reaction with IOTs SCMs system. Due to the effect of TEA on CH crystallization, more amorphous CH is produced.

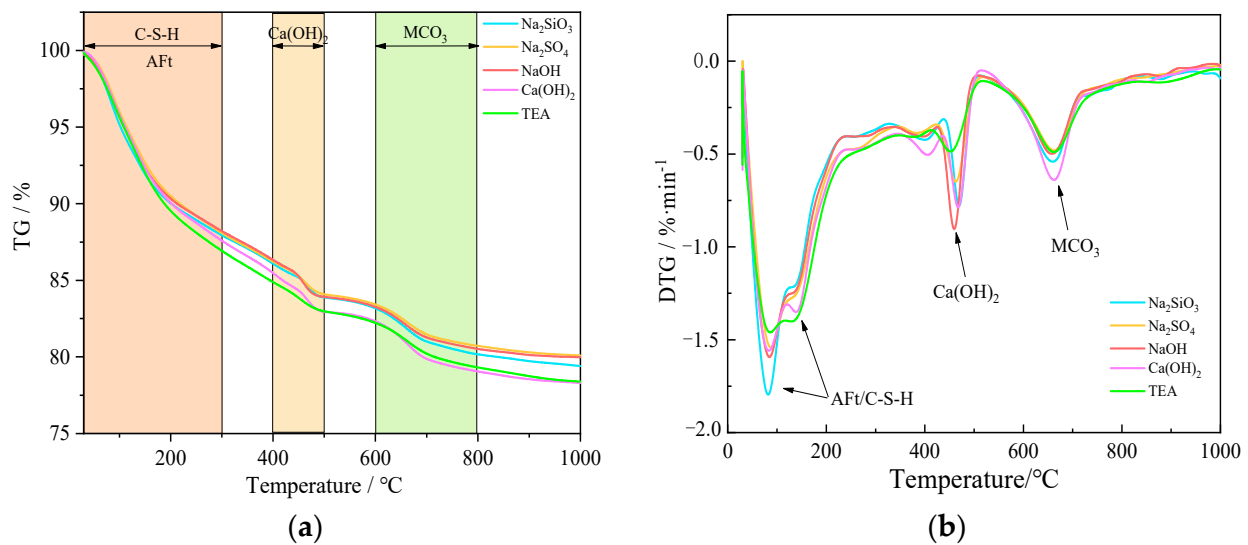


**Figure 5.** TG–DTG curves of different mechanical–chemical coupling activation modes at 28 days: (a) TG curves; (b) DTG curves.

**Table 3.** Content of non-evaporated water and  $\text{Ca(OH)}_2$  of hydration products under different chemical admixtures.

Serial Number	Dehydrated Amount of Aft, C-S-H/C-(A)-S-H	Dehydrated Amount of CH	$\text{CaCO}_3$ Amount of Decomposition	Total Loss	$\text{Ca(OH)}_2$ Content
$\text{Na}_2\text{SiO}_3$	8.92%	2.92%	3.01%	20.6%	20.8%
$\text{Na}_2\text{SO}_4$	8.92%	2.81%	2.7%	19.9%	19.68%
NaOH	8.92%	3.07%	2.73%	20.0%	19.82%
$\text{Ca(OH)}_2$	9.34%	3.15%	3.27%	21.6%	22.28%
TEA	9.53%	2.66%	2.90%	21.7%	19.41%

### 3.5. MIP Analyses

The performance of mortar mainly depends on the pore structure, and MIP is often considered the main method for pore structure analysis. In this section, pore structure analysis was conducted on three samples: OPC, no-chemical-additive day 28 sample (IOTs), and the TEA-added day 28 sample (TEA-IOTs). Table 4 shows the pore structure parameters and porosity of the samples at 28 days via MIP. At 28 days, the total porosity of these samples was lower than that of the OPC samples, with TEA-IOTs showing the lowest porosity (23.2%) compared to IOTs (25.6%) and OPC (28%). This reduction in porosity corresponds to the observed improvements in the macroscopic mechanical strength of the samples. Additionally, Figure 6 indicates that the pore distribution curves of TEA-IOTs and IOTs samples shift to the right, suggesting that the high-silica iron tailing-based composite dopant refines pores larger than 50 nm, increases the number of 2–50 nm pores, and optimizes the deleterious pore structure. As shown in Table 4, the IOTs samples exhibited fewer less harmful and harmful pores compared to the TEA-IOTs samples. This is attributed to the “microaggregate effect” of high-silica iron tailings composite dopants, which enhance the hardening system through physical filling. Additionally, materials like steel slag and steel tailings contribute to the hardening process. Steel slag and slag contribute additional  $\text{Ca}^{2+}$  and  $\text{OH}^-$  ions, which facilitate the dissolution of alumina in fly ash and activate  $\text{C}_2\text{S}$  and  $\text{C}_3\text{S}$  in the steel slag. This leads to the production of more calcite and C-(A)-S-H gel through the consumption of  $\text{Ca(OH)}_2$ . Consequently, the reduction in free water around the hydration products results in fewer harmful pores, thereby enhancing

the hydration process and leading to the formation of more pores around these hydration products. Furthermore, the presence of pores larger than 20 nm in the three samples aligns with TG analysis findings. An increase in these larger pores suggests enhanced reactions between atmospheric  $\text{CO}_2$  and C-(A)-S-H gel or  $\text{Ca}(\text{OH})_2$ , leading to the formation of additional carbonate products.

**Table 4.** Pore structure parameters and porosity of the specimens at 28 days via MIP.

Serial Number	Pore Size Distribution mL/g				Porosity
	<20 nm	20–50 nm	50–200 nm	>200 nm	
OPC	0.07000	0.00764	0.00574	0.00002	28%
IOTs	0.16220	0.01523	0.00030	0.00001	25.6%
TEA-IOTs	0.12514	0.01856	0.00051	0.00001	23.2%

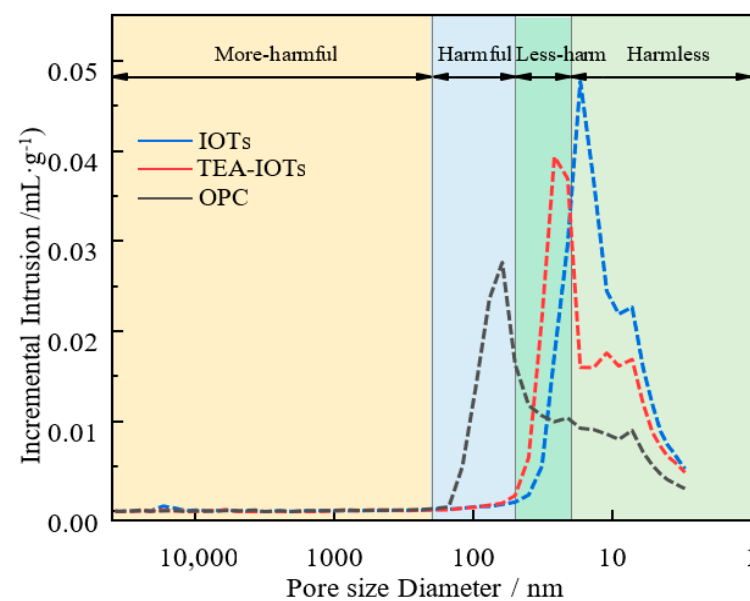


**Figure 6.** Pore size distribution of different samples.

### 3.6. SEM Analyses

SEM is capable of analyzing the morphological characteristics of hydration products and thus clarifying the structure and type of hydration products. Figure 7 displays the SEM images of samples chemically activated for 28 days. A large number of honeycomb-like C-(A)-S-H gels and a small number of lamellar AFt crystals, intertwined with each other and lapped, were present in the composite admixture. Attached to the unreacted slag particles and SS, the particles were tightly cemented together to form a dense whole, so that the strength of the composite admixture increased significantly. The un-hydrated steel slag particles also played a micro-filling role in the composite admixture. There were also a large number of hexagonal flakes of un-hydrated  $\text{Ca}(\text{OH})_2$  in the composite admixture system, which could maintain the alkalinity of the admixture and enable the hydration reaction to continue. Different reaction degrees and sizes of steel slag particles can also promote the continued hydration of slag, so with the increase of the age of maintenance, the compressive strength of the composite admixture is also gradually increased. The presence of  $\text{CaCO}_3$  was also observed in the SCMs, which, due to the presence of  $\text{Ca}(\text{OH})_2$  and SS in the SCMs, would lead to the carbonation of the material to generate  $\text{CaCO}_3$  during preparation and maintenance. This would not only act as a filler of the pores of the composites, but also provide nucleation sites for the gels, and thus promote the generation of C-(A)-S-H gels.

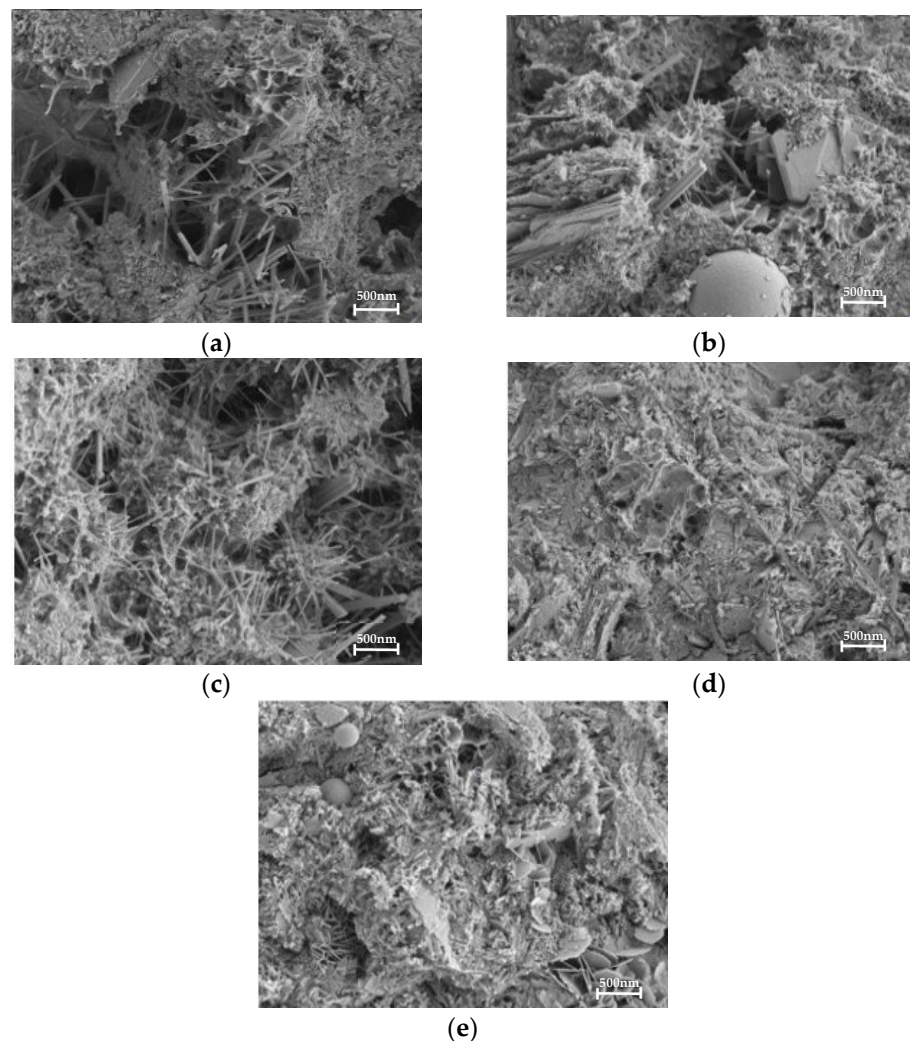


**Figure 7.** 28 days' SEM results of chemical activation: (a) Na<sub>2</sub>SiO<sub>3</sub> activate; (b) Na<sub>2</sub>SO<sub>4</sub> activate; (c) NaOH activate; (d) Ca(OH)<sub>2</sub> activate; (e) TEA activate.

## 4. Discussion

### 4.1. Mechanism of Mechanical-Chemical Activation Coupling

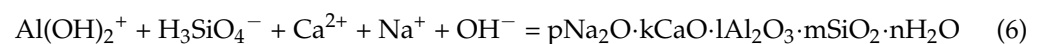
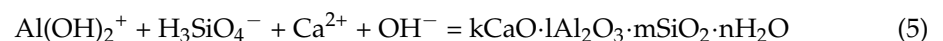
The results show that mechanochemical activation increases the activity and better improves the performance, which is similar to the results of previous studies. It has been shown that there is an increase in disordered material in IOTs powder, and the addition of IOTs powder promotes the secondary hydration of the aluminum phase of cement, which significantly improves the cementitious activity, in the presence of mechanochemical coupling [34].

IOTs are inert materials and require mechanical or chemical activation to increase the potential activity of the material and thus enhance the rate of hydration within the system. The sample's surface undergoes mutual extrusion and collision deformation due to the combined effects of mechanochemical grinding and crystal surface energy. This results in the fracture of chemical bonds. Due to the Si-O bonding effect at the end of the powder, the fractured surface of the powder becomes charged. Adsorption and polymerization, resulting in the formation of new Si-O-Si or O-Si-O bridge bonds, will take place between the cross-sections. The appearance of cracks on the surface and inside the crystal structure, and the irregular changes in the crystal surface, make the lattice deformation different, including deformation and dislocation. Simultaneously, the polar water molecules and dispersed OH ions provided by the chemical activator penetrate the internal pores of the crystal structure, interact with the active cations, diffuse and dissolve IOTs, and facilitate

the nucleation, growth, and overlapping of hydrates. Thus, a dense microstructure is formed. Increasing the activator content and grinding time results in a rapid reaction, larger product particle size, and looser crystal overlap, leading to decreased strength.

#### 4.2. Analysis of the Mechanism of Action of Chemical Activation

Inorganic chemical activators have a certain stimulating effect on the activity of iron tailings-based composite admixtures. The results of the current study show that the chemical components in steel slag and fly ash are more in between glassy, where the main chemical bonds are Si-O and Al-O and exist as  $\text{SiO}_4$  tetrahedra,  $\text{AlO}_4$  tetrahedra, and  $\text{AlO}_6$  coordination polyhedra, respectively, in their vitreous forms. When  $\text{Na}_2\text{SiO}_3$ ,  $\text{Na}_2\text{SO}_4$ , and  $\text{NaOH}$  are present, the coordination number of  $\text{Si}^{4+}$  is four for  $\text{SiO}_4$  tetrahedra, each  $\text{Si}^{4+}$  is attached to  $4\text{O}^{2-}$ , and each  $\text{O}^{2-}$  is attached to  $2\text{Si}^{4+}$ . Vitreous bodies form through reacting in the alkaline environment formed by chemical activators. Similarly,  $\text{AlO}_4$  depolymerizes to  $\text{H}_3\text{AlO}_4^{2-}$  under the action of  $\text{OH}^-$ .  $\text{H}_3\text{AlO}_4^{2-}$  is able to react with  $\text{H}_3\text{SiO}_4^-$ ,  $\text{Ca}^{2+}$ , and  $\text{Na}^+$  to form zeolite-like products, as shown in Equations (3) and (4). Zeolite-like products have a very low solubility, and the continuous generation of zeolite-like products continuously consumes the depolymerized  $\text{H}_3\text{SiO}_4^-$  and  $\text{H}_3\text{AlO}_4^{2-}$ , prompted by the steel slag vitreous Si-O and Al-O chemical bond rupture.  $\text{Na}_2\text{SiO}_3$  is more alkaline than  $\text{Na}_2\text{SO}_4$ , and in addition to the hydration process to provide  $\text{OH}^-$  and  $\text{Na}^+$ , it can also provide  $\text{Si}^{4+}$ , so the same amount of  $\text{Na}_2\text{SiO}_3$  chemical activator adds to a higher compressive strength. In addition to this,  $\text{Na}_2\text{SiO}_3$  in water glass has a very high degree of depolymerization, which can act as a skeleton so that the hydration products, such as C-(A)-S-H gel, generated by the dopant reaction become embedded and fill in its skeleton, which further improves the strength of the steel slag cementitious system. Similarly, when  $\text{NaOH}$  and  $\text{Ca}(\text{OH})_2$  are added to the iron tailings-based composite admixture, they will likewise provide an alkaline hydration environment for it, creating conditions for the depolymerization of  $\text{SiO}_4$  tetrahedra and  $\text{AlO}_4$  tetrahedra in the steel slag vitreous body, which in turn promotes strength enhancement. In contrast to alkaline excitors, salt excitors provide additional  $\text{SiO}_4^{2-}$  while maintaining an alkaline hydration environment, resulting in a better excitation effect.



The activation effect of TEA is also related to the dosage. Under the suitable dosage, it can promote the hydration process of the dopant so that its hydration is sufficient. But more than the optimal yield, the acceleration of its hydration process is preferred, resulting in the structure around the hydration product becoming looser, which reduces the densification of the system, and leads to the reduction of strength. The inclusion of TEA has a beneficial impact on the initial strength development of pure silicate cement systems, but it reduces their later strengths. However, the presence of volcanic ash-active SCMs alters or even reverses this decrease, leading to an increase in strength [30]. Specifically, the major contributors to the decrease in strength are the changes in hydration products, especially the decomposition of AFt and the formation of AFm. In the initial period, TEA promoted the formation of more AFt to improve strength. TEA accelerates the dissolution and hydration of  $\text{C}_3\text{A}$  and  $\text{C}_4\text{AF}$ , while prolonging the induction period and hindering the hydration of  $\text{C}_3\text{S}$  [35]. The IOTs SCMs system had lower amounts of clinker minerals and gypsum than the pure PC system, which resulted in a lower amount of AFt formed in the early period, and a reduced effect on strength as fewer AFm products can be formed. In an IOTs SCMs system, the volcanic ash reaction and cement hydration are represented simultaneously and continuously. TEA prevents the process of crystalline nucleation of hydration products through complexation, thereby inhibiting the hydration of silicate minerals. The high

fineness of SCMs provides nucleation sites for hydration products, which may counteract the inhibition of  $C_3S$  by TEA. Moreover, TEA is easily adsorbed on the surface of CH and precipitated with CH in solution, which affects the nucleation and growth of CH. The addition of TEA decreases the content of crystalline CH and increases the content of amorphous and non-crystalline CH, which can enter the hydration product C-S-H, which may represent one of the reasons why TEA promotes the volcanic ash reaction [36]. TEA consistently improved the compressive strength of the IOTs SCMs system, both in the early and late periods, mainly because TEA greatly facilitated the reaction of cement minerals and the pozzolanic reaction of SCMs. The results confirm that the interaction between the complexation reaction of TEA and the volcanic ash reaction is a valuable contribution to the development of cement strength.

TEA doses above 1% significantly reduced the compressive strength of IOTs after 28 days. The silicate reaction was significantly impeded by two main factors. Firstly, the over-addition of TEA directly slowed down the hydration process of  $C_3S$ , possibly due to the formation of a Ca-TEA complex layer on the surface of the  $C_3S$  phase, the dissolution of  $C_3S$ , and the nucleation of C-S-H during the later stage were impeded [37]. Conversely, for the silicate reaction, the inclusion of TEA significantly enhanced the hydration of aluminates, which subsequently delayed the hydration process of  $C_3S$  [38]. The over-addition of TEA alters the rate-controlling process of OPC hydration from being dominated by silicate reactions to being dominated by aluminate reactions. This change inhibits the strength development in the later stages of hydration in hydrated OPC systems.

## 5. Conclusions

This paper presents a study on the strengthening of IOTs SCMs using different chemical activation methods. In this regard, the chemical activator dosage effect, compressive strength, hydration products, pore structure, and the mechanism of activation of IOTs SCMs were studied in this paper. The above experimental results and discussion lead to the following conclusions:

- (1) Compared to the five chemical additives, TEA maximized the compressive strength of IOTs SCMs. When TEA is used at a 1% dosage, it increases the strength of IOTs at 7 days to 28.6 MPa, and at 28 days to 42.9 MPa, comparable to OPC 42.5.
- (2) SCMs provide additional nucleation sites for hydration products. The addition of TEA enhances the amount of amorphous and non-crystalline CH in the system, thereby promoting the reaction of volcanic ash and counteracting the inhibitory effect of TEA on  $C_3S$ . The interaction of the TEA complexation reaction with the volcanic ash reaction represents the main reason for the positive development of the late strength of IOTs SCMs.
- (3) The use of the chemical additive in the IOTs reduces the harmful pores and carbonate content in the cement samples. Chemical activation of the IOTs has impacted the optimization of both non-damaging and damaging porosities. This activation process revitalizes the hydration process, leading to more rapid hydration and increased pore formation around the hydration products, thereby affecting the optimization of pore structures.

Based on the summary above, the addition of chemical additives can improve the working performance of SCM, among which TEA can promote the volcanic ash reaction, thus improving the gelling activity of IOTs and increasing its consumption. This is essential for expanding the consumption of IOT in the cement and concrete industries. Therefore, this study provides a fundamental basis for strengthening IOTs SCMs.

**Author Contributions:** Conceptualization, Z.H. and X.G. (Xiaowei Gu); methodology, J.L., B.C. and Q.W.; validation, X.G., S.Y. and Z.H.; formal analysis, Z.H.; investigation, B.C. and S.Y.; resources, X.G. (Xiaowei Ge) and B.C.; data curation, Z.H.; writing—original draft preparation, Z.H.; writing—review and editing, Q.W.; visualization, X.G. (Xiaowei Ge); supervision, X.G. (Xiaowei Gu); project administration, Q.W. and J.L.; funding acquisition, X.G. (Xiaowei Gu). All authors have read and agreed to the published version of the manuscript.

**Funding:** This research was funded by the National Key Research and Development Plan of China grant number No. 2023YFC3904303, the National Natural Science Foundation of China grant number No. 52234004, and the Social Governance Special Project of Shenyang Municipal Bureau of Science and Technology grant number No. 22-322-3-02. Special thanks to Shiyanjia Lab ([www.shiyanjia.com](http://www.shiyanjia.com), accessed on 16 December 2022) for providing technical analysis.

**Data Availability Statement:** The original contributions presented in the study are included in the article, further inquiries can be directed to the corresponding author.

**Conflicts of Interest:** The authors declare that there are no conflicts of interest regarding the publishing of this paper.

## References

1. Zhang, N.; Tang, B.; Liu, X. Cementitious activity of iron ore tailing and its utilization in cementitious materials, bricks and concrete. *Constr. Build. Mater.* **2021**, *288*, 123022. [[CrossRef](#)]
2. Zhang, Y.; Li, Z.; Gu, X.; Nehdi, M.L.; Marani, A.; Zhang, L. Utilization of iron ore tailings with high volume in green concrete. *J. Build. Eng.* **2023**, *72*, 106585. [[CrossRef](#)]
3. Li, Y.; Sheng, J.; Li, W.; Yu, M.; Zheng, X.; Wang, F. Effect of a novel spherical tailings aggregate on the macro- and mesoscopic properties of pervious concrete. *Cem. Concr. Compos.* **2023**, *144*, 105311. [[CrossRef](#)]
4. Zhao, S.; Fan, J.; Sun, W. Utilization of iron ore tailings as fine aggregate in ultra-high performance concrete. *Constr. Build. Mater.* **2014**, *50*, 540–548. [[CrossRef](#)]
5. Shettima, A.U.; Hussin, M.W.; Ahmad, Y.; Mirza, J. Evaluation of iron ore tailings as replacement for fine aggregate in concrete. *Constr. Build. Mater.* **2016**, *120*, 72–79. [[CrossRef](#)]
6. Manjunatha, M.; Seth, D.; Kvgd, B.; Roy, S.; Tangadagi, R.B. Utilization of industrial-based PVC waste powder in self-compacting concrete: A sustainable building material. *J. Clean. Prod.* **2023**, *428*, 139428. [[CrossRef](#)]
7. Xiang, J.; Qiu, J.; Zhao, Y.; Zheng, P.; Peng, H.; Fei, X. Rheology, mechanical properties, and hydration of synergistically activated coal gasification slag with three typical solid wastes. *Cem. Concr. Compos.* **2024**, *147*, 105418. [[CrossRef](#)]
8. Liu, K.; Wang, S.; Quan, X.; Jing, W.; Xu, J.; Zhao, N.; Liu, B.; Ying, H. Industrial byproduct Iron ore tailings as ecofriendly materials in the utilization of cementitious composites. *Constr. Build. Mater.* **2023**, *372*, 130813. [[CrossRef](#)]
9. Lothenbach, B.; Scrivener, K.; Hooton, R.D. Supplementary cementitious materials. *Cem. Concr. Res.* **2011**, *41*, 1244–1256. [[CrossRef](#)]
10. Zhang, Y.; Zhang, L.; Wang, Q.; Han, D.; Li, Z. Iron ore tailings, phosphate slags, and lithium slags as ternary supplementary cementitious materials for concrete: Study on compression strength and microstructure. *Mater. Today Commun.* **2023**, *36*, 106644. [[CrossRef](#)]
11. Durdziński, P.T.; Ben Haha, M.; Bernal, S.A.; De Belie, N.; Gruyaert, E.; Lothenbach, B.; Menéndez Méndez, E.; Provis, J.L.; Schöler, A.; Stabler, C.; et al. Outcomes of the RILEM round robin on degree of reaction of slag and fly ash in blended cements. *Mater. Struct.* **2017**, *50*, 135. [[CrossRef](#)]
12. Scrivener, K.L.; Juilland, P.; Monteiro, P.J.M. Advances in understanding hydration of Portland cement. *Cem. Concr. Res.* **2015**, *78*, 38–56. [[CrossRef](#)]
13. Almada, B.S.; Alves da Silva Neto, G.; Fraga do Prado, D.; Paulino Aguilar, M.T.; Silva Garcia, D.C.; Brigolini Silva, G.J.; José dos Santos, W. Evaluation of the microstructure and micromechanics properties of structural mortars with addition of iron ore tailings. *J. Build. Eng.* **2023**, *63*, 105405. [[CrossRef](#)]
14. Cheng, Y.; Huang, F.; Li, W.; Liu, R.; Li, G.; Wei, J. Test research on the effects of mechanochemically activated iron tailings on the compressive strength of concrete. *Constr. Build. Mater.* **2016**, *118*, 164–170. [[CrossRef](#)]
15. Liu, B.; Meng, H.; Pan, G.; Zhou, H.; Li, D. Relationship between the fineness and specific surface area of iron tailing powder and its effect on compressive strength and drying shrinkage of cement composites. *Constr. Build. Mater.* **2022**, *357*, 129421. [[CrossRef](#)]
16. Duarte, M.S.; Almada, B.S.; José dos Santos, W.; Lima Bessa, S.A.; Cesar da Silva Bezerra, A.; Paulino Aguilar, M.T. Influence of mechanical treatment and magnetic separation on the performance of iron ore tailings as supplementary cementitious material. *J. Build. Eng.* **2022**, *59*, 105099. [[CrossRef](#)]
17. Goulart Bezerra, C.; Abelha Rocha, C.A.; Siqueira, I.S.d.; Toledo Filho, R.D. Feasibility of iron-rich ore tailing as supplementary cementitious material in cement pastes. *Constr. Build. Mater.* **2021**, *303*, 124496. [[CrossRef](#)]
18. Liu, J.; Ge, X.; Liu, P.; Song, G.; Hu, Z. Experimental study on the preparation of cementitious materials from iron ore tailings by activation. *Constr. Build. Mater.* **2023**, *385*, 131409. [[CrossRef](#)]

19. Yang, Y.; Yang, Z.; Cheng, Z.; Zhang, H. Effects of wet grinding combined with chemical activation on the activity of iron tailings powder. *Case Stud. Constr. Mater.* **2022**, *17*, e01385. [[CrossRef](#)]
20. Carvalho, A.R.d.; Calderón-Morales, B.R.d.S.; Borba Júnior, J.C.; Oliveira, T.M.d.; Silva, G.J.B. Proposition of geopolymers obtained through the acid activation of iron ore tailings with phosphoric acid. *Constr. Build. Mater.* **2023**, *403*, 133078. [[CrossRef](#)]
21. Cheah, C.B.; Tan, L.E.; Ramli, M. Recent advances in slag-based binder and chemical activators derived from industrial by-products—A review. *Constr. Build. Mater.* **2021**, *272*, 121657. [[CrossRef](#)]
22. Xu, Z.; Li, W.; Sun, J.; Hu, Y.; Xu, K.; Ma, S.; Shen, X. Research on cement hydration and hardening with different alkanolamines. *Constr. Build. Mater.* **2017**, *141*, 296–306. [[CrossRef](#)]
23. Teng, Y.; Liu, S.; Zhang, Z.; Xue, J.; Guan, X. Effect of triethanolamine on the chloride binding capacity of cement paste with a high volume of fly ash. *Constr. Build. Mater.* **2022**, *315*, 125612. [[CrossRef](#)]
24. He, Y.; Liu, S.; Zhang, X.; Liu, W.; Liao, G.; Xu, M. Influence of triethanolamine on mechanical strength and hydration performance of blended cement containing fly ash, limestone and slag. *J. Build. Eng.* **2021**, *44*, 102879. [[CrossRef](#)]
25. Heren, Z.; Ölmez, H. The influence of ethanolamines on the hydration and mechanical properties of portland cement. *Cem. Concr. Res.* **1996**, *26*, 701–705. [[CrossRef](#)]
26. Cheung, J.; Jeknavorian, A.; Roberts, L.; Silva, D. Impact of admixtures on the hydration kinetics of Portland cement. *Cem. Concr. Res.* **2011**, *41*, 1289–1309. [[CrossRef](#)]
27. Ghafari, E.; Ghahari, S.; Feys, D.; Khayat, K.; Baig, A.; Ferron, R. Admixture compatibility with natural supplementary cementitious materials. *Cem. Concr. Compos.* **2020**, *112*, 103683. [[CrossRef](#)]
28. Kourounis, S.; Tsivilis, S.; Tsakiridis, P.E.; Papadimitriou, G.D.; Tsihouki, Z. Properties and hydration of blended cements with steelmaking slag. *Cem. Concr. Res.* **2007**, *37*, 815–822. [[CrossRef](#)]
29. Yang, X.; Wu, S.; Xu, S.; Chen, B.; Chen, D.; Wang, F.; Jiang, J.; Fan, L.; Tu, L. Effects of GBFS content and curing methods on the working performance and microstructure of ternary geopolymers based on high-content steel slag. *Constr. Build. Mater.* **2024**, *410*, 134128. [[CrossRef](#)]
30. Jiang, J.; Ye, Z.; Wu, J.; Yang, Q.; Li, Q.; Kong, X. Impact of triethanolamine on the hydration of Portland cement in the presence of high pozzolanic activity supplementary cementitious materials. *Cem. Concr. Compos.* **2024**, *147*, 105435. [[CrossRef](#)]
31. Ilić, B.; Radonjanin, V.; Malešev, M.; Zdujić, M.; Mitrović, A. Effects of mechanical and thermal activation on pozzolanic activity of kaolin containing mica. *Appl. Clay Sci.* **2016**, *123*, 173–181. [[CrossRef](#)]
32. Zhang, Y.; Liu, B.; Gu, X.; Nehdi, M.L.; Zhang, L.V. Mechanochemical activation of iron ore tailing-based ternary supplementary cementitious materials. *Constr. Build. Mater.* **2022**, *346*, 128420. [[CrossRef](#)]
33. Saeki, T.; Monteiro, P.J.M. A model to predict the amount of calcium hydroxide in concrete containing mineral admixtures. *Cem. Concr. Res.* **2005**, *35*, 1914–1921. [[CrossRef](#)]
34. Piao, C.; Wang, D.; Zhang, L.; Wang, C.; Liu, H. Influence of chemical mechanical coupling effect on iron ore tailings cementitious activity. *Yingyong Jichu Yu Gongcheng Kexue Xuebao/J. Basic Sci. Eng.* **2016**, *24*, 1100–1109. [[CrossRef](#)]
35. Han, J.; Wang, K.; Shi, J.; Wang, Y. Mechanism of triethanolamine on Portland cement hydration process and microstructure characteristics. *Constr. Build. Mater.* **2015**, *93*, 457–462. [[CrossRef](#)]
36. Zhang, Y.R.; Kong, X.M.; Lu, Z.C.; Lu, Z.B.; Qing, Z.; Dong, B.Q.; Feng, X. Influence of triethanolamine on the hydration product of portlandite in cement paste and the mechanism. *Cem. Concr. Res.* **2016**, *87*, 64–76. [[CrossRef](#)]
37. Ramachandran, V.S. Influence of triethanolamine on the hydration characteristics of tricalcium silicate. *J. Appl. Chem. Biotechnol.* **1972**, *22*, 1125–1138. [[CrossRef](#)]
38. Lu, Z.; Kong, X.; Jansen, D.; Zhang, C.; Wang, J.; Pang, X.; Yin, J. Towards a further understanding of cement hydration in the presence of triethanolamine. *Cem. Concr. Res.* **2020**, *132*, 106041. [[CrossRef](#)]

**Disclaimer/Publisher’s Note:** The statements, opinions and data contained in all publications are solely those of the individual author(s) and contributor(s) and not of MDPI and/or the editor(s). MDPI and/or the editor(s) disclaim responsibility for any injury to people or property resulting from any ideas, methods, instructions or products referred to in the content.